# Finite Element Analysis of Indented Pipes Using Two-dimensional Solid Elements

**Oliveira Jr, Silvestre Carvalho**
**UFC – Centro de Tecnologia – Campus do Pici, Bloco 714**
**e-mail – silvestre@metalmat.ufc.br**

**Deus, Enio Pontes**
**UFC – Centro de Tecnologia – Campus do Pici, Bloco 714**
**e-mail – epontes@ufc.br**

***Abstract.*** *Mechanical damage in the form of dents on pipes has deserved thorough investigation so far. Not only do the offshore industry have concerned about the subject, but it has also attracted a lot of attention in the providing water companies. By virtue of that, this paper presents a numerical analysis of indented pipes based on the Finite Element (FE) within the framework of the software Comsol. Numerical models using two-dimensional solid plane strain elements are evaluated. Moreover, geometric nonlinear analysis, nonlinear isotropic hardening material and contact were incorporated into the models. In addition, a mesh sensitivity analysis is also carried out. Due to symmetry only a half of the pipe and indenter were analyzed. The following topics were studied during indentation: force-deflection diagram on unpressurized and pressurized pipes, elastic recovery after removing the indenter with variation in the internal pressure loading. Furthermore, limit loads were also investigated for unpressurized pipes. Different pipes geometries and material are used. The numerical models are calibrated by either using analytical or experimental model from scientific communities.*

***Keywords****: Pipe indentation, Finite Element Analysis*

## 1. INTRODUCTION

Tubular members have been widely used for transporting water, oil, gas and sewage as well. For this reason, professionals from oil industry or providing water companies are constantly worried about the durability of the pipes, because they are often subjected to heavy loads, which may cause significant damage, (Karamanos *et al*, 2006). Specifically, dents are a typical mechanical damage which has been effected on its structural integrity through all the years. For this reason, detailed numerical analyses and also experimental work have described the behavior of this type of damage, (Seng *et al,* 1989), (Ong *et al*, 1992). Specifically, they can be caused by falling objects such as anchors, trawl gears, excavation equipment, earth movement and rock, (Pichler *et al*, 2005). Moreover, the most severe common form of dents are due to a presence of gouges, (MacDonald *et al*, 2007). Generally, they reduce both static and cyclic strength of the pipes, (Ávila, 2007).

The main objective of this work is to investigate the performance of indented pipes under variation of some geometrical parameters such as dent's depth (d), diameter (D) and thickness (t), Fig. 1 and also the internal pressure loading or unpressurized pipes. In addition the mechanism of elastic recovery after removing the indenter will be also analysed. Herein, the pressure is applied as long as the indentation force is applied.

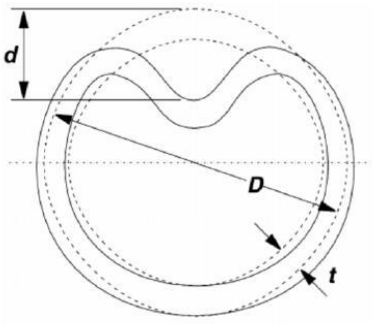


Figure 1. Indentation geometric parameters

A numerical model based on Finite Element Model was developed within the framework of the software *Comsol*, (Comsol 3.4 Version Manual, 2005). The effects of indenter's form and presence of others defects such as gouges or cracks were not investigated through FE model, (Blachut and Iflefel, 2007). Two different materials were used in the FE analysis. Specifically, the calibration of the model was based on the experimental results of the 6082-T6 aluminum alloy, (Hyde *et al,* 2005). The X60 steel was also used in order to use a practical pipe material.

The aluminum or steel layer are assumed to be J2-type elastic-plastic, finitely deforming solid with isotropic hardening. The indenter is modeled as a rigid material and there is also a rigid base at the bottom of the pipe. Contacts among the indenter, pipe and rigid base are also considered. Figure 2 shows the indenter, pipe and rigid base.

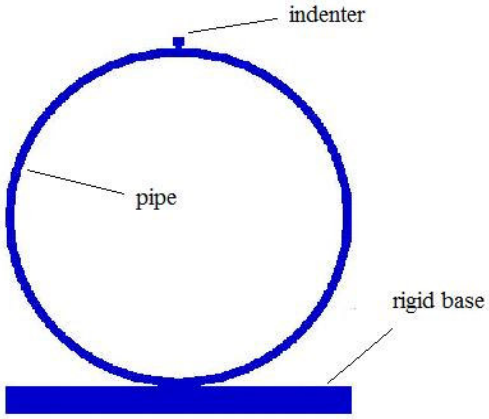


Figure 2. Dented pipe set on a rigid base.

## 2. GEOMETRY

For the numerical models, pipes made of metal were set on a rigid base whose length is the same size of the external diameter of the pipe and thickness of 10mm. The pipe was simply supported on a node located at the angular position of $45^o$ , Fig. 3a, (Hyde *et al*, 2005). Symmetry conditions reduces the problem to one half of the original geometry, Fig. 3b. The force per unit length of the pipe was monitored at the top of the indenter.

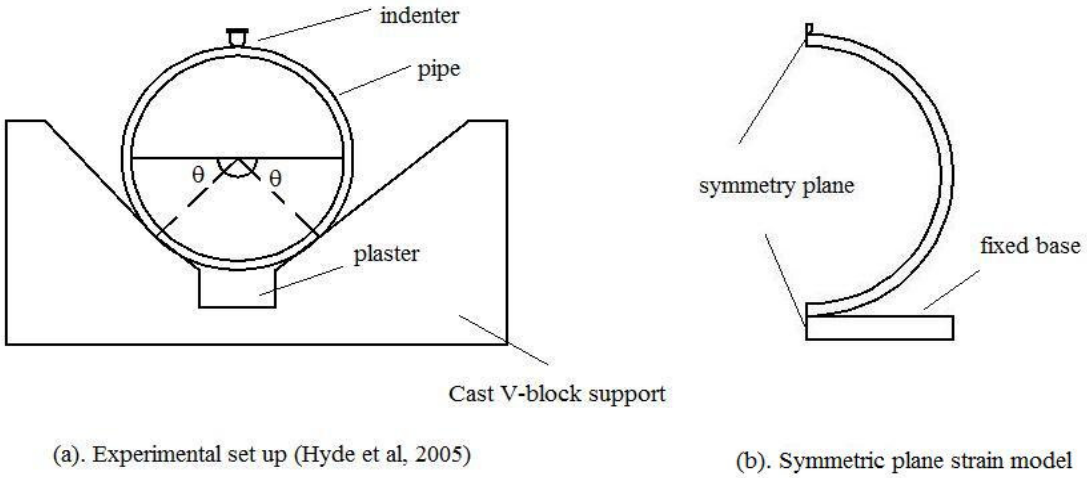


(a). Experimental set up (Hyde et al, 2005)

(b). Symmetric plane strain model

Figure 3. Experimental set up and numerical model

The nomenclature used to identify the different types of geometry is represented by the name PIPEX, where X represents the D/t (diameter/thickness) ratios. It will be also used the nomenclature FE which means Finite Element. Table 1 shows the main geometric parameters of the pipe , where D is the external diameter and t is the thickness.

Table 1. Main geometric parameters of the pipes analysed.

| Specimen | D (mm) | t (mm) | D/t |
|---|---|---|---|
| PIPE24 | 120 | 5 | 24 |
| PIPE31 | 92 | 3 | 31 |
| PIPE42 | 125 | 3 | 42 |
| PIPE74 | 89 | 1.2 | 74 |

## 3. MATERIAL

The elastic properties of the 6082-T6 aluminum alloy is showed in Tab. 2, where E represents the Young modulus, $\sigma_Y$ is the yield stress and $\sigma_{UTS}$ is the ultimate nominal tensile stress. The plastic part was modeled as a non linear-hardening isotropic material. The properties of the X60 steel were also showed in Table 2 and the stress-strain curve were obtained in (Oliveira Jr *et al,* 2005). Figure 4 also shows the true stress-strain curves of both materials.

Table 2. Mechanical properties of 6082-T6 Aluminum and X60 Steel.

| Material Properties | 6082-T6 Aluminum | X60 Steel |
|---|---|---|
| E (MPa) | 70000 | 206820 |
| $\sigma_Y$ (MPa) | 300 | 485 |
| $\sigma_{UTS}$ (MPa) | 351 | 574 |

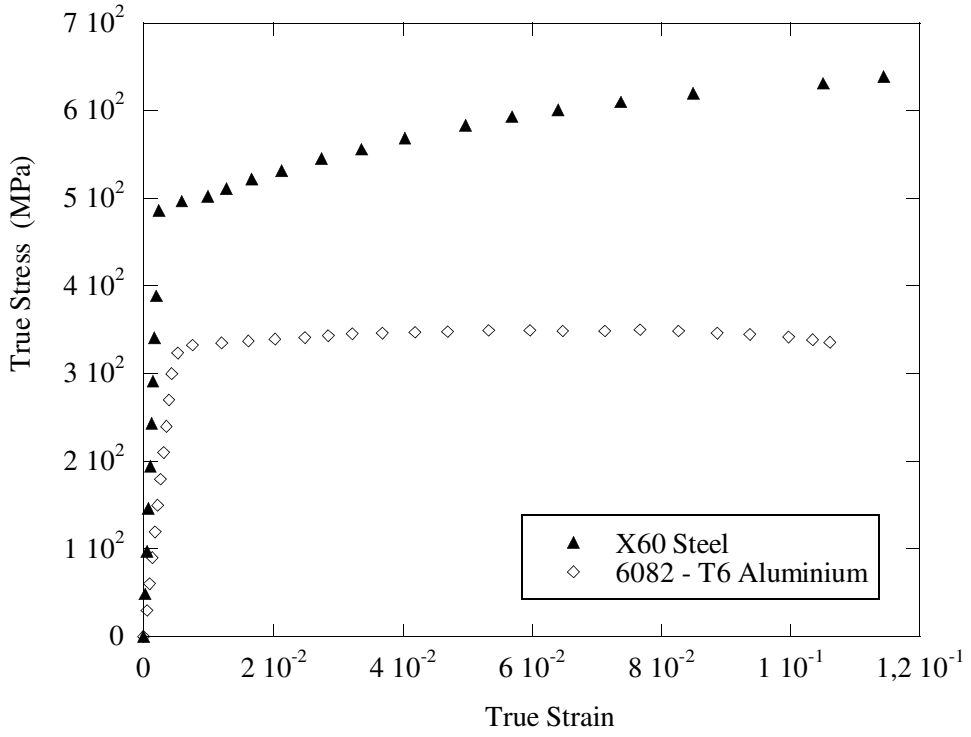


Figure 4. True stress-strain curves of 6082-T6 aluminum alloy and X60 Steel.

## 4. ANALYTICAL FORMULATION

The initial objective of the FE analysis was to compare the model based on the experimental results and analytical expressions of unpressurized pipes performed in (Hyde *et al*, 2005), where the symmetric pipe, Fig. 3b, is supported in a node at an angle of $\theta=45^o$. The analytical solutions derived in (Hyde *et al*, 2005) for unpressurized pipes, so as to predict the force-deflection response is based on the linear beam theory using energy conservation principle with small deformations. Furthermore, the ring was fully fixed at the cross section at the angular support, Fig. 3a. Equation (1) shows the analytical expression of the initial gradient. Therefore, the variables involved into Eq. (1) are E (Young Modulus), t (thickness of the pipe), R (radius of the pipe) and D its diameter.

$$Ke=(E*t^3/12*R^3)*D/(A*D+B+C) \quad (1)$$

Where the coefficients A, B, C and D are functions of the angular position $\Theta$, as in Eq. (2), Eq. (3), Eq. (4) and Eq. (5).

$$A=(\pi/2+\theta+\sin(2*\theta))/4 \quad (2)$$

$$B=(1+sen(\theta))*(1.5*sen(2*\theta)+3*\cos(\theta)-(0.5*\pi+\theta)*(\cos(\theta)^2+sen(\theta)+1)) \quad (3)$$

$$C=\cos(\theta)*(1/2+sen(\theta)^2/2+sen(\theta))*((\pi/2+\theta)*\cos(\theta)-2*sen(\theta)-2) \quad (4)$$

$$D=2*((\pi/2+\theta)^2-2*\cos(\theta)^2-(\pi/2+\theta)*sen(2*\theta)/2) \quad (5)$$

By means of the analytical expression evaluated by (Hyde *et al*, 2005), it is also calculated the limit load for unpressurized dented rings. The equation was developed using upper bound theorems (Chen, 1988) and it is represented by the equation below.

$$Panal(\sigma)=0.25*(\sigma*t^2/R)*(1+sen(\theta)/2*sen(\pi/4+\theta/2)-\cos(\theta)) \quad (6)$$

Where the variable θ is the same described in Eq. (1), R is the average radius of the pipe. The variable σ will be represented by means of three different variables, $\sigma_Y$ (yield stress), $\sigma_{UTS}$ (ultimate tensile stress) and $\sigma_F$ (flow stress) which the most commonly expression is represented by the Eq. (7), (Ong *et al*, 1992).

$$\sigma_F=0.5*(\sigma_Y+\sigma_{UTS}) \quad (7)$$

## 5. NUMERICAL ANALYSIS

A numerical model based on the finite element method was developed within the framework of the software *COMSOL,* so as to simulate the behavior of indented pipes. Eight-nodes, quadratic, two-dimensional element, with two degree-of-freedom per node (displacements in 1 and 2 directions) were used to model the assembly. The pipe was discretized with 734 elements and the region near the indenter was more refined (560 elements), Fig. 5. The plane strain model is frictionless, geometric nonlinearity and nonlinear hardening isotropic material. This model allows the validation of contact between rigid and flexible bodies. A load force is applied on the rigid indenter and causes the pipe deformation that comes into contact with the second rigid base at the bottom. Two contact pairs are defined, one between the rigid indenter and the flexible pipe and other between the flexible pipe and the rigid base.

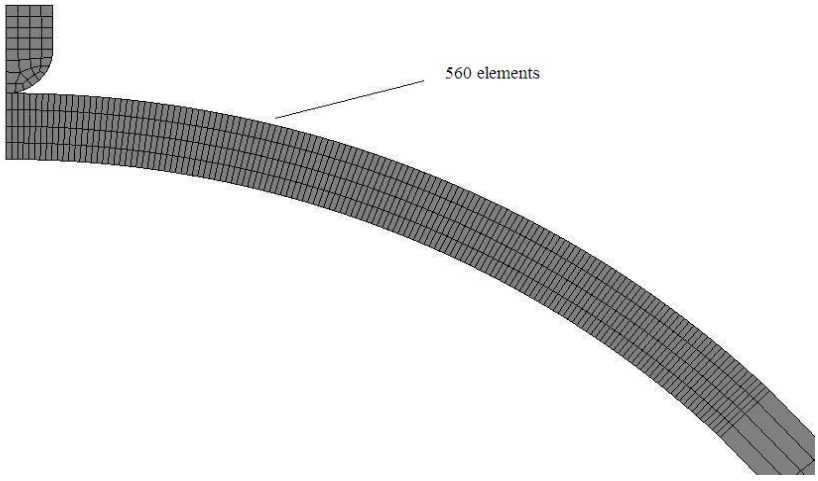


Figure 5. FE mesh in the region of the indentation used in the indented pipe analysis.

### 5.1. Initial Gradient

The initial gradient is obtained from the slope of the curve of indentation force versus dent depth as it shown in Fig. 6 for unpressurized pipes. Furthermore, it is also obtained the peak loads (limit loads) from the same previous curve.

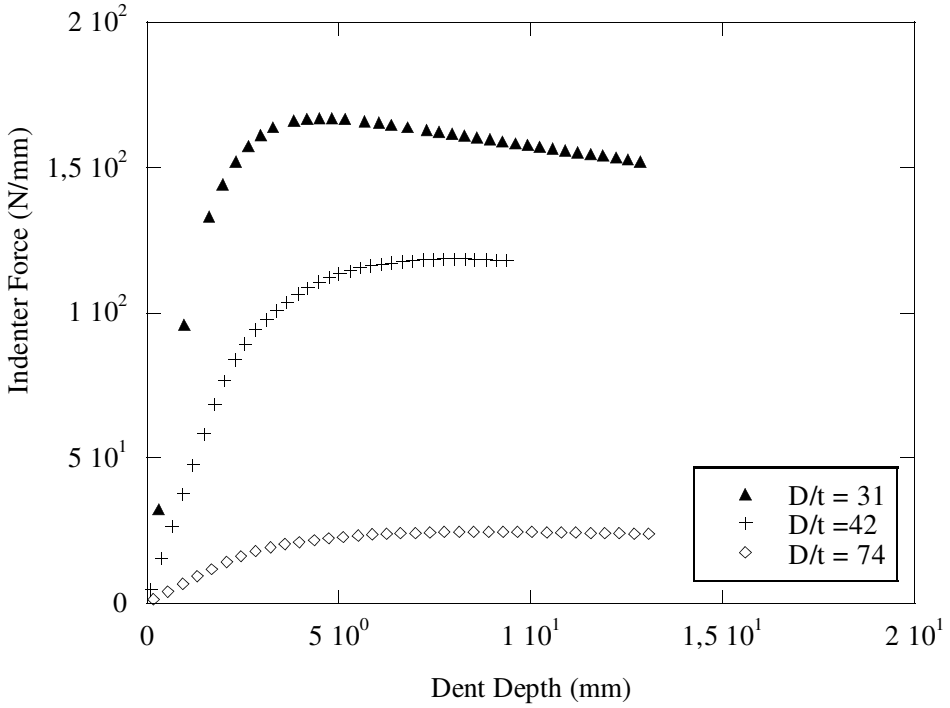


Figure 6. Typical indenter force versus dent's depth curves from FE analyses for X60 steel pipes.

Table 3 shows the results based on the initial gradient which is obtained from the force (per unit length of the pipe) versus dent depth curve, where Kexp and Kanalit represents the average initial gradient experimental and analytical initial gradient, respectively (Hyde *et al*, 2005) and Knum represents initial gradients of the numerical models. As it is seen in Tab. 3, for larger D/t ratios the numerical results are approximated to experimental and analytical ones. On the other hand, for D/t < 30, the numerical and analytical results also tends to be well-matched. Nevertheless, the experimental results showed to be more conservative. For X60 steel pipes, the correlation numerical-analytical also showed to be effective, Tab. 4.

Table 3. Comparison of the initial gradient results for support angle at $\theta = 45^o$ (6082-T6 Aluminum).

| Specimen | D (mm) | t (mm) | D/t | Kexp (MPa) | Knum (MPa) | Kanalit (MPa) |
|---|---|---|---|---|---|---|
| PIPE24 | 120 | 5 | 24 | 61.40 | 72.50 | 71 |
| PIPE31 | 92 | 3 | 31 | 23.60 | 34.40 | 34 |
| PIPE42 | 125 | 3 | 42 | 10.80 | 13.60 | 14 |
| PIPE74 | 89 | 1.2 | 74 | 2.30 | 2.40 | 2.42 |

Table 4. Comparison of the initial gradient results for support angle at $\theta = 45^o$ (X60 Steel).

| Specimen | D (mm) | t (mm) | D/t | Knum (MPa) | Kanalit (MPa) |
|---|---|---|---|---|---|
| PIPE24 | 120 | 5 | 24 | 215 | 210 |
| PIPE31 | 92 | 3 | 31 | 102 | 99 |
| PIPE42 | 125 | 3 | 42 | 40.20 | 40 |
| PIPE74 | 89 | 1.2 | 74 | 7 | 7.15 |

For pressurized pipes, there is a couple effect between internal pressure and the indentation force on the displacement caused by the combined load, (Crisfield, 1991). Additionally, this pressure causes initial deflections and stresses within the pipe. Hence,this phenomenon causes an initial force on the curve Indenter Force versus dent depth, It worths mentioning that this value also increases as long as the pressure increase.

It is clear that the pressure has a large influence on the Initial Gradient of the numerical models. Under the same pressure, the required indenter force, here represented by initial gradient, increases as the pressure also increases. However, it is likely that the pipe becomes stiffer as long as the pressure becomes larger. In addition, the difference of the required force between a lowly pressurized pipe and a highly pressurized pipe increases as the D/t ratio is lower. For D/t equals to 74 (thinner pipes) the initial gradient ratio between X60 steel and Aluminum pipes decreases from 3,0 to 1,41 as the pressure goes from 0 to 10 MPa. Otherwise, this relation has a smaller decrease from 3,0 to 1,61 for D/t equal to 42 (thicker pipes) at the same interval of pressure, Fig. 7.

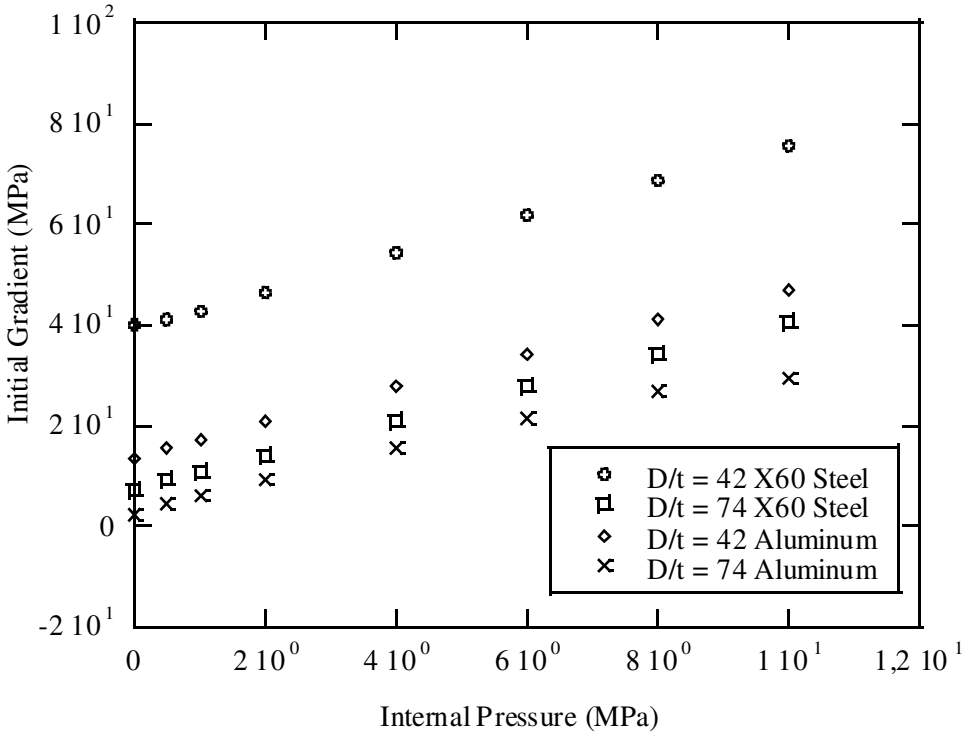


Figure 7. Initial Gradient versus internal pressure from FE analysis for different D/t ratios and materials.

### 5.2. Elastic Recovery

The process of introducing a dent into a pipe involves elastic and plastic deformations. However, when the indenter is removed the dent will spring back to some degree (elastic recovery). In addition, the dent depth changes as the internal pressure increases. Moreover, this effect can rely on some parameters such as pipe geometry, material properties and also the presence of internal pressure, PDAM (Pipeline Defect Assessment Manual) recommends the Eq. (8), (Cosham and Hopkins, 2004).

$$dr(PDAM) = dmax/1.43 \tag{8}$$

Where dmax is the dent depth at zero pressure and dr is dent depth at pressure remaining after damage (after spring back). (Ávila, 2007) describes thoroughly whose parameters are involved in the PDAM criterion . Hereafter, the intention of the value of dr (PDAM) is only to compare to the numerical results. It is also supposed that when the dent is formed, the pipe is internally pressurized. Therefore, for the numerical models, the internal pressure is applied as soon as indentation force is applied. Moreover, PDAM presents a considerable view of the best currently available methods for the assessment of pipeline defects, such as corrosion, dents, gouges, weld defects and so on, (Cosham and Hopkins, 2004).

Figure 8 shows a typical indenter force versus dent depth for X60 steel Pipe74. It clearly shows that there is a predominant increase of the initial stiffness as the pressure increases. Nevertheless, the level of stress inside the pipe is so intense that causes the rupture of the pipe. It is characterized by the interruption of the curve, where the iteration process starts diverging and no more solution is found.

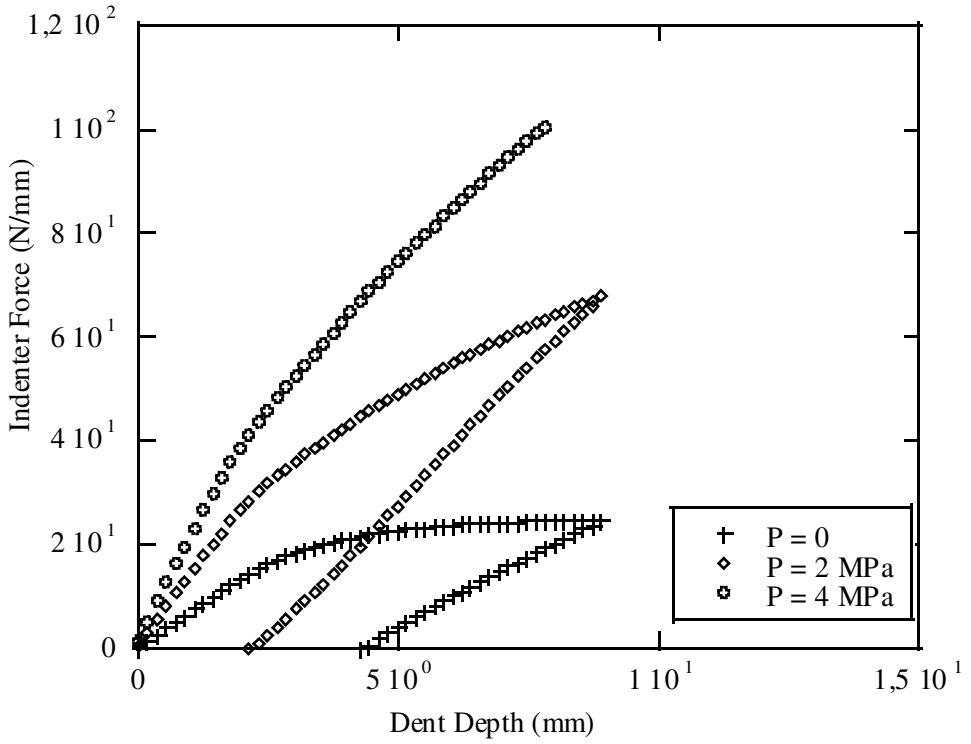


Figure 8. Indenter force versus dent depth curves of X60 steel Pipe74.

Table 5 shows the numerical results based on the dent depth after spring back (dr), dr (PDAM), P (internal pressure) and RR (recovery ratio) which is the relation between dr (numerical spring back) and dmax (maximum depth of the pipe). The (*) values in Tab. 5 means that the pipe has failed before reaching the maximum depth, thereby the numerical iteration process starts diverging.

It is seen that dents introduced into pressurized pipes springs back more than dents introduced into unpressurized pipes at the same maximum depth. In addition, for unpressurized pipes, dents in thinner walled pipes also springs back more than dents in thicker walled pipes,where RR varies from 0.48 (Pipe74) to 0.8 (Pipe24). Conversely, for pressurized pipes, it is noteworthy that the internal pressure causes less recovery (RR) at the same D/t ratio.

It is also observed in Tab. 5 that the values of the dent depth after spring back of PDAM, Eq. (8) tends to be more conservative, chiefly, when the pipe is pressurized. On the other hand, for unpressurized pipes, the numerical results (dr) are in good agreement with the Eq. (8), as long as the thickness increases.

A great number of pressurized pipes has failed before they reached the maximum depth, as it showed in Tab. 5 (*).

Table 5. Numerical spring back value (dr), dr (PDAM) and RR.

| Specimen | D/t | dmax (mm) | P (MPa) | dr (mm) | dr (PDAM) | RR |
|---|---|---|---|---|---|---|
| Pipe74 | 74 | 10%D | 0 | 4.26 | 6.21 | 0.48 |
| | | | 2 | 2.13 | | 0.24 |
| | | | 4 | * | | * |
| | | | 6 | * | | * |
| | | | 8 | * | | * |
| | | | 10 | * | | * |
| Pipe42 | 42 | 10%D | 0 | 8.5 | 8.74 | 0.68 |
| | | | 2 | 7.0 | | 0.56 |
| | | | 4 | * | | * |
| | | | 6 | * | | * |
| | | | 8 | * | | * |
| | | | 10 | * | | * |
| Pipe31 | 31 | 10%D | 0 | 6.91 | 6.46 | 0.75 |
| | | | 2 | 6.47 | | 0.70 |
| | | | 4 | 5.91 | | 0.64 |
| | | | 6 | 5.36 | | 0.58 |
| | | | 8 | 4.62 | | 0.50 |
| | | | 10 | 4.07 | | 0.44 |
| Pipe24 | 24 | 10%D | 0 | 9.6 | 8.39 | 0.80 |
| | | | 2 | * | | * |
| | | | 4 | * | | * |
| | | | 6 | * | | * |
| | | | 8 | * | | * |
| | | | 10 | * | | * |

### 5.3. Limit Loads

Tables 6 and 7 show the solutions for limit loads for 6082-T6 aluminum and X60 steel pipes for unpressurized pipes, respectively, where Pexp represents the experimental limit load performed by (Hyde *et al,* 2005), Pnum is the numerical limit load obtained by FEM analysis and the variables Panal ($\sigma_Y$) Panal ($\sigma_F$) and Panal ($\sigma_{UTS}$) represent the analytical limit load formulation, (Hyde *et al*, 2005), using yield stress, flow stress, Eq. (7) and ultimate tensile stress, respectively, into Eq. (6), as described in item 4. The numerical limit loads were obtained from the maximum point of the curve indentation force versus dent depth.

Table 6. Solutions for limit loads for 6082-T6 Aluminum pipes.

| Specimen | D/t | Pexp (N/mm) | Pnum (N/mm) | Panalit($\sigma_Y$) (N/mm) | Panalit($\sigma_F$) (N/mm) | Panalit($\sigma_{UTS}$) (N/mm) |
|---|---|---|---|---|---|---|
| PIPE24 | 24 | 204 | 223.45 | 195.20 | 211.80 | 228.40 |
| PIPE31 | 31 | 87.40 | 102 | 90.40 | 98.10 | 105.80 |
| PIPE42 | 42 | 63.50 | 71.50 | 66.30 | 71.90 | 77.50 |
| PIPE74 | 74 | 14 | 14.3 | 14.80 | 16 | 17.30 |

Table 7. Solutions for limit loads for X60 Steel pipes.

| Specimen | D/t | Pnum (N/mm) | Panalit($\sigma_Y$) (N/mm) | Panalit($\sigma_F$) (N/mm) | Panalit($\sigma_{UTS}$) (N/mm) |
|---|---|---|---|---|---|
| PIPE24 | 24 | 369 | 315.80 | 344.50 | 373.20 |
| PIPE31 | 31 | 167.10 | 146.20 | 159.50 | 172.80 |
| PIPE42 | 42 | 118.50 | 107.20 | 116.90 | 126.60 |
| PIPE74 | 74 | 24.5 | 23.90 | 26 | 28 |

For smaller D/t ratios ranging from 24 to 42, the limit loads obtained from the experiments showed in Table 6 for 6082-T6 aluminum tends to be more conservative in relation to the limit loads obtained from the FE analysis. In addition, it is also showed in Tab. 6 that the FE results and analytical limit loads are consistent. Moreover, it seems that using the flow stress in the analytical formulation gives closer correlation numerical-analytical results in relation to the limit loads. Likewise, the same conclusion can be made in relation to the correlation numerical-analytical solutions for limit loads for X60 steel pipes, Tab. 7

## 6. CONCLUSIONS

The indentation on pressurized and unpressurized pipes was evaluated through a FE analysis. Experimental and analytical results from scientific communities were used to calibrate the models. The numerical results of the pipes based on the initial gradients are in good agreement with the analytical model proposed by (Hyde *et al*, 2005) for aluminum and X60 steel pipes. But, the experimental results of the aluminum pipes were more conservative than the numerical models as soon as the D/t ratio increases. The numerical models also showed that the initial gradient increases as soon as the pressure increases.

The numerical models were also used to study the elastic recovery of the pipes after indentation. The pipeline defect assessment manual (PDAM) was used to compare to the numerical results based on the dent depth after spring back (dr). Equation (8) tends to be more conservative, chiefly, when the pipe is pressurized. On the other hand, for unpressurized pipes, the numerical results (dr) are in good agreement with the Eq. (8), as long as the thickness increases. It was also observed that a great number of pipes had failed under internal pressure before, they reached the maximum depth. It is also necessary to carry out a detailed experimental program and also more numerical results.

The numerical limit loads were also investigated in relation to the analytical formulation performed by (Hyde *et al*, 2005). However, for 6082-T6 aluminum, the experimental limit load (Pexp) tends to be more conservative in relation to the numerical limit loads (Pnum). Furthermore, the analytical limit loads using flow stress in the analytical formulation, (Hyde *et al*, 2005) give a good agreement in relation to the numerical limit loads results (Pnum). Similarly, the comparison among limit loads results for X60 steel.

## 7. ACKNOWLEDGEMENTS

The authors would like to acknowledge the financial support from National Counsel of Technological and Scientific Development (CNPq) and Fundação Cearense de Apoio ao Desenvolvimento Científico (Funcap).

## 8. REFERENCES

Ávila, M.A.V., 2007, “Structural Integrity of Plain Dents in Pipelines”, Master of Science Dissertation, Departamento de Engenharia Mecânica, Pontifícia Universidade Católica do Rio de Janeiro, pp. 1-196.

Blachut, J., Iflefel, I. B., 2007, “Collapse of Pipes with Plain or Gouge Dents by Bending Moment”, , International Journal of Pressure Vessel & Piping, Vol. 84, pp. 560-571.

Chen, W.F., 1988, “Plasticity for Structural Engineers”, Berlin Springer.

Comsol Manual, 2005, “Comsol Multiphysics User's Guide”, Version 3.4, pp. 1-622.

Cosham, A., Hopkins, P., 2004, “The effect of dents in Pipelines – Guidance in the Pipeline Defect Assessment Manual“, International Journal of Pressure Vessels & Piping, Vol. 81, pp. 127-139.

Crisfield, M.A., 1991, “Non-linear Finite Element Analysis of Solids and Structures”, Vol.1, Chichester, Wiley.

Hyde, T. H., Luo, R and Becker, A. A., 2005, “Elastic-plastic Response of Unpressurized Pipes Subjected to Axially-Long Radial Indentation"”, International Journal of Mechanical Sciences, Vol. 47, pp. 1949-1971.

Karamanos, A.S.Andreadakis, K.P., 2006, “Denting of Internally Pressurized Tubes Under Lateral Loads”, International Journal of Mechanucal Sciences, Vol. 48, pp. 1080-1094.

Macdonald, K. A., Cosham, A., Alexander, C. R. and Hopkins, P., 2007, “Assessing Mechanical Damaging in Offshore Pipelines – Two case studies”, Engineering Failure Analysis, Vol.14, pp. 1667-1679.

Oliveira Jr, S. C., Netto, T.A. and Pasqualino, I.P., 2005, “Metal-Composite Pipes for Deepwater Applications", Proceedings of the 18th International Congress of Mechanical Engineering, Vol. 1, Ouro Preto, Brazil.

Ong, L.S., Soh, A.K. and Ong, J.H., 1992,”Experimental and Finite Element Investigation of a Local Dent on a Pressurized Pipe”, Journal of Strain Analysis, Vol. 27, pp. 177-185.

Pichler, B., Hellmich, C., Eberhardsteiner, J. and Mang, H.A., 2005, “Assessment of Protection Systems for Buried Steel Pipelines Endangered by Rockfall”, Vol. 20, pp. 331-342.

Seng, O.L., Wing, C.Y and Seet, G., 1989, “he Elastic Analysis of a Dent on Pressurized Pipe”, International Journal of Pressure Vessel & Piping, Vol.38, pp. 369-383.

## 9. RESPONSIBILITY NOTICE

The author(s) is (are) the only responsible for the printed material included in this paper.